

Theory of polar scattering in semiconductor quantum structures

B. A. Mason* and S. Das Sarma[†]

Center for Theoretical Physics, Department of Physics and Astronomy, University of Maryland, College Park, Maryland 20742

(Received 10 June 1986; revised manuscript received 7 November 1986)

The scattering rate of free electrons due to polar interactions with LO phonons in two-dimensional structures (e.g., semiconductor heterojunctions and quantum wells) is calculated as a function of the electron energy, electron and lattice temperatures, the carrier density, and the layer thickness. A many-body perturbative formalism is used with phonon-emission and -absorption self-energy terms obtained explicitly. Effects of screening and degeneracy on the scattering rate are critically discussed. Detailed numerical results for the experimentally well-studied modulation-doped GaAs heterojunctions and quantum wells are given.

I. INTRODUCTION

Two-dimensionally confined electron systems in semiconductor heterojunctions and quantum wells have been (and are being) intensively¹ studied both theoretically and experimentally in the last few years. Our goal in this paper is to provide a fairly detailed theoretical picture for the electron-LO-phonon-interaction-induced polar scattering of free carriers in these systems. Our numerical results will concentrate on electron systems based on GaAs-Al_xGa_{1-x}As structures; however, a rough quantitative estimate for hole scattering can be obtained by a simple scaling of the electron-phonon coupling constant. Even though all numerical results presented in this paper are for two-dimensionally confined electrons in GaAs structures (both heterojunctions and quantum wells), trends and qualitative conclusions we make should be approximately valid in other similar polar two-dimensional structures like HgTe-CdTe, InAs-GaSb, Ga_{1-x}In_xAs-InP, and Ga_{1-x}In_xAs-Al_{1-y}In_yAs systems. Our reason for concentrating on GaAs-Al_xGa_{1-x}As structures is the simple fact that it is by far the most extensively studied system. This system also has the advantage of being simple in its electronic band structure where the model of isotropic and parabolic two-dimensional dispersion of electron energy in each subband is an accurate approximation.

The motivation for our work is almost obvious. Many of the electronic properties of heterojunctions and quantum wells are expected to be modified by electron-LO-phonon scattering via the Fröhlich interaction. In fact, there already exists a substantial body of literature dealing with the electron-optical-phonon interaction in two-dimensional structures including a number of our own publications.²⁻⁷ Polaronic renormalization of carrier effective mass in two dimensions due to the electron-phonon interaction has been considered in a number of recent papers, both experimentally⁸ and theoretically.⁹ Of more relevance to this work are a number of papers,¹⁰⁻¹² notably by Price¹⁰ and by Ridley,¹¹ that deal with the scattering rate and transport contributions by the electron-LO-phonon interaction in two-dimensional structures. Where appropriate, our results reduce to these results. There have also been a number of mobility calculations^{12,10} in GaAs-Al_xGa_{1-x}As and other related structures where the electron-LO-phonon scattering contribu-

tion (mostly from the absorption of phonons, which becomes important at higher temperatures, $T > 100$ K) is implicitly included. Room-temperature mobility in modulation-doped GaAs heterostructures is thought to be mainly limited by LO-phonon scattering; however, it is not easy to separate out contributions from various terms (e.g., charged-impurity scattering, scattering by remote dopants, acoustic-phonon scattering, alloy scattering) to the transport data, since Mathiessen's rule is not valid at high temperatures.

One important category of experiments to which electron-LO-phonon scattering considerations of this paper are directly relevant is the hot-electron energy-loss study. A number of experimental papers with somewhat conflicting results have appeared on this subject in the recent literature.¹³⁻¹⁷ Our belief is that a complete quantitative theory for these experiments is difficult and, at the present time, nonexistent. Results presented in this paper enable one to make some semiquantitative conclusions about the basic mechanism of electron-phonon interaction underlying these hot-electron studies. Trends in our electron-phonon scattering-rate results are consistent with those observed in the experiment and any remaining discrepancy should be attributed to physical mechanisms explicitly excluded in our theory (e.g., hot-phonon effect¹⁸). But the fact that the experimental results from different groups are in disagreement with each other clearly precludes any definite conclusion on this subject based on our calculations. Electron-LO-phonon interaction in two-dimensional systems has also been studied in the context of calculations of subband structure and optical properties by various authors.¹⁹

The model we employ for our calculation is that of a two-dimensional electron gas of areal number density N_s confined to the *lowest* quantum subband of a semiconductor heterojunction or single quantum well interacting with the *dispersionless bulk* LO phonons of the host semiconductor (e.g., GaAs in the Al_xGa_{1-x}As system) via the continuum Fröhlich Hamiltonian.^{2,20} We assume the two-dimensional energy dispersion of these electrons to be *parabolic* and isotropic.

The *effective-mass approximation* is assumed to be valid uncritically and any subtle effect arising from the bulk band structure of the system is completely ignored (this clearly limits the quantitative validity of the theory when

applied to hole systems which have complicated band structure). The model we employ here has been extensively used²¹ in the study of two-dimensional electron systems and, even though fairly simple, it is expected to be quite accurate for electrons two dimensionally confined in the conduction subbands of GaAs in GaAs-Al_xGa_{1-x}As heterostructures. More details on the theoretical model and on our approximations are given in the next section of the paper and in Ref. 2. In Sec. III we discuss the static screening model and in Sec. IV we present and discuss our numerical results for the polar scattering rate of electrons in GaAs-Al_xGa_{1-x}As heterojunctions and quantum wells as functions of *all* the relevant physical parameters of the system (e.g., temperature, electron density, well thickness) and for a number of different approximation schemes as explained in Secs. II and III. We conclude in Sec. V with a summary of our results, a critique of the various approximations used in this work, and a critical discussion

of our view of the experimental and theoretical status of the subject.

II. THEORY, MODEL, AND APPROXIMATIONS

The central quantity we calculate in this paper, under various approximation schemes, is the leading-order electronic self-energy correction due to polar-electron-LO-phonon interaction via the Fröhlich Hamiltonian. Details of the formalism are standard and have already been given in Ref. 2. We omit the formal details, except to state that our interest in this paper is to obtain the imaginary part of the electronic self-energy which is related directly to the single-particle broadening and scattering rates, and indirectly to electronic mobility and hot-electron relaxation rate. The imaginary part of the unscreened self-energy can be written in the leading order in α , the Fröhlich coupling constant,²⁰ as ($\hbar=1$ throughout this paper)

$$\text{Im}\Sigma(k, E) = -\frac{\alpha\omega_{\text{LO}}^{3/2}}{2(2m)^{1/2}} \int_0^\infty dq f(q) \int_0^{2\pi} d\theta \{ [n_B + n_F(\mathbf{k}-\mathbf{q})]\delta(E + \omega_{\text{LO}} - E_0(\mathbf{k}-\mathbf{q})) \\ + [n_B + 1 - n_F(\mathbf{k}-\mathbf{q})]\delta(E - \omega_{\text{LO}} - E_0(\mathbf{k}-\mathbf{q})) \}, \quad (1)$$

where we have explicitly taken into account the two-dimensional isotropy of the model, noting that the self-energy depends only on the magnitude $k = |\mathbf{k}|$ of the electron wave vector, and E is a general energy variable. In Eq. (1) α , ω_{LO} , and m are, respectively, the bulk Fröhlich coupling constant for polar interaction (in GaAs), LO-phonon frequency, and the electronic band effective mass. The two-dimensional wave vectors \mathbf{k} and \mathbf{q} are, respectively, the electron and phonon wave vectors in the plane of the layer, whereas θ is the scattering angle in the plane defined by

$$|\mathbf{k}-\mathbf{q}| \equiv (k^2 + q^2 - 2kq \cos\theta)^{1/2}.$$

The quantity $E_0(k) = k^2/2m$ is the bare electronic energy with all band nonparabolicity effects neglected uncritically (this should be valid for GaAs systems at not overly high electron densities). The functions n_B and n_F are Bose and Fermi occupation factors defined by

$$n_B \equiv (e^{\beta\omega_{\text{LO}}} - 1)^{-1}$$

and

$$n_F(k) \equiv (e^{\beta[E_0(k) - \mu]} + 1)^{-1},$$

where μ , the chemical potential, is determined from the total electron density N_s of the system, and $\beta = (k_B T)^{-1}$. Finally, $f(q)$ is the electronic form factor² associated with the subband quantization in the z direction and its form for both the heterojunction and the quantum-well situations are well known^{2,21} and are given in the Appendix for the sake of completeness. The self-energy is an explicit function of the independent variables k and E , and contains more information than a scattering rate which is a function of k only [or, equivalently, of $E_0(\mathbf{k})$]. For example, the damping of an electronic state is given by $\text{Im}\Sigma$, and, as such, it is related to the tunneling rate²² and to the quasiparticle lifetime.²³ In this paper, however, we are interested in the polar scattering rate $\Gamma(k)$ for the quasiparticle and, therefore, we calculate $\text{Im}\Sigma(k, E)$ on the “mass shell” by substituting $E = k^2/2m \equiv E_0(\mathbf{k})$ in Eq. (1):

$$\Gamma(k) \equiv -\text{Im}\Sigma(k, E = k^2/2m) \\ = \frac{\alpha\omega_{\text{LO}}^{3/2}}{2(2m)^{1/2}} \int_0^\infty dq f(q) \int_0^{2\pi} d\theta \{ [n_B + n_F(\mathbf{k}-\mathbf{q})]\delta(E_0(\mathbf{k}) + \omega_{\text{LO}} - E_0(\mathbf{k}-\mathbf{q})) \\ + [n_B + 1 - n_F(\mathbf{k}-\mathbf{q})]\delta(E_0(\mathbf{k}) - \omega_{\text{LO}} - E_0(\mathbf{k}-\mathbf{q})) \}. \quad (2)$$

The first term in Eq. (2) denotes a LO-phonon absorption by the electron, whereas the second term denotes the emission of a LO phonon. It is customary to discuss free-carrier scattering by LO phonons in terms of absorption and emission processes and we divide the total damping rate of Eq. (2) into an absorption part Γ_a and an emission part Γ_e :

$$\Gamma_a(k) = \frac{\alpha\omega_{\text{LO}}^{3/2}}{2(2m)^{1/2}} \int_0^\infty dq f(q) \int_0^{2\pi} d\theta [n_B + n_F(\mathbf{k}-\mathbf{q})]\delta(E_0(\mathbf{k}) + \omega_{\text{LO}} - E_0(\mathbf{k}-\mathbf{q})), \quad (3)$$

$$\Gamma_e(k) = \frac{\alpha\omega_{\text{LO}}^{3/2}}{2(2m)^{1/2}} \int_0^\infty dq f(q) \int_0^{2\pi} d\theta [n_B + 1 - n_F(\mathbf{k}-\mathbf{q})] \delta(E_0(\mathbf{k}) - \omega_{\text{LO}} - E_0(\mathbf{k}-\mathbf{q})) . \quad (4)$$

The dependence of the absorption and emission rates in Eqs. (3) and (4) on the electron energy E_0 is easily obtained by noting that $k = (2mE_0)^{1/2}$. We want to emphasize that Γ_a is nonzero even when $n_B = 0$ (e.g., very low temperatures). This is entirely due to the existence of a Fermi surface in the problem (i.e., because $n_F \neq 0$) which allows a “quasihole” inside the Fermi surface to decay by the emission of a LO phonon, and the emission of a LO phonon by a quasihole is equivalent to the absorption of a LO phonon by the quasielectron. In fact, the absorption term in Eq. (3) can be thought of as an emission process for quasiholes and the equivalence between the terms inside the square brackets in Eqs. (3) and (4) becomes clear when one notes that the Fermi occupancy factor for holes (n_H) is given by $n_H = (1 - n_F)$. We shall not pursue this discussion any further here, except to note that for a cou-

pled electron-phonon system, where a degenerate electron gas is interacting with a phonon field, the conceptual distinction between absorption and emission of phonons becomes somewhat obscure because of the existence of both electrons and holes as quantiparticles in the Fermi sea. We point out that with the mass-shell approximation $E = E_0(k)$ in Eq. (1), the calculation now becomes equivalent to Fermi’s golden rule—type theory for the scattering rate with quantum statistics effect explicitly retained in Eq. (2).

The integrations over the scattering angle θ in Eqs. (3) and (4) are straightforward to carry out using the fact that

$$\begin{aligned} \delta(E_0(\mathbf{k}) \pm \omega_{\text{LO}} - E_0(\mathbf{k}-\mathbf{q})) \\ = \delta(kq \cos\theta / m - q^2 / 2m \pm \omega_{\text{LO}}) , \end{aligned}$$

and we get

$$\Gamma_a(k) = (\alpha\gamma\omega_{\text{LO}}) [n_B + n_F(k^2 + \gamma^2)^{1/2}] \int_{-k + (k^2 + \gamma^2)^{1/2}}^{k + (k^2 + \gamma^2)^{1/2}} dq f(q) [4k^2q^2 - (q^2 - \gamma^2)^2]^{-1/2} \quad (5)$$

and

$$\Gamma_e(k) = (\alpha\gamma\omega_{\text{LO}}) H(k - \gamma) [1 + n_B - n_F(k^2 - \gamma^2)^{1/2}] \int_{k - (k^2 - \gamma^2)^{1/2}}^{k + (k^2 - \gamma^2)^{1/2}} dq f(q) [4k^2q^2 - (q^2 + \gamma^2)^2]^{-1/2} , \quad (6)$$

where

$$\gamma^2 = 2m\omega_{\text{LO}} \quad (7)$$

and

$$n_F(k^2 \pm \gamma^2)^{1/2} = (1 + e^{\beta(k^2/2m \pm \omega_{\text{LO}} - \mu)})^{-1} , \quad (8)$$

with $n_B = (e^{\beta\omega_{\text{LO}}} - 1)^{-1}$ as usual. The chemical potential μ of the electrons is determined by the electron density N_s and the absolute temperature T :

$$\mu = \beta^{-1} \ln(e^{\beta E_F} - 1) , \quad (9)$$

where

$$E_F = \pi N_s / m \quad (10)$$

is the Fermi energy [$E_F = \mu(T=0)$] of the system. The Heaviside unit step function $H(x)$ in Eq. (6) is simply 0 or 1, depending on whether $x < 1$ or $x > 1$, respectively.

For a *strictly two-dimensional system* the subband form factor $f(q)$ is unity and the q integration in Eqs. (5) and (6) can then be performed analytically. We get

$$\Gamma_a^{(2D)}(k) = (\alpha\gamma\omega_{\text{LO}}) [n_B + n_F(k^2 + \gamma^2)^{1/2}] (k^2 + \gamma^2)^{-1/2} K(k / (k^2 + \gamma^2)^{1/2}) , \quad (11)$$

$$\Gamma_e^{(2D)}(k) = (\alpha\gamma\omega_{\text{LO}}) [n_B + 1 - n_F(k^2 + \gamma^2)^{1/2}] k^{-1} H(k - \gamma) K((k^2 - \gamma^2)^{1/2} / k) , \quad (12)$$

where

$$K(x) = \int_0^{\pi/2} d\phi (1 - x^2 \sin^2\phi)^{-1/2}$$

is the complete elliptic integral of the first kind and the superscript indicates that we are considering the purely two-dimensional limit. In fact, we can get a fairly accurate *analytic* approximation to the polar scattering rate in the actual quasi-two-dimensional electron layer by noting that the form factor $f(q)$ is a rather slowly varying func-

tion of the wave vector q and can, therefore, be taken out of the integral with its value being evaluated at the average wave vector. Thus we can evaluate the integrals in Eqs. (5) and (6) approximately as

$$\Gamma_a(k) \approx \Gamma_a^{(2D)}(k) f(k^2 + \gamma^2)^{1/2} , \quad (13)$$

$$\Gamma_e(k) \approx \Gamma_e^{(2D)}(k) f(k) , \quad (14)$$

where $\Gamma_{a,e}^{(2D)}(k)$ are the strictly two-dimensional scattering

rates given by Eqs. (11) and (12). Using the fact that the electron energy E_0 is related to the wave vector k by the relation $E_0 = k^2/2m$, one can obtain the dependence of phonon emission and absorption rates on the electron energy (E_0) from Eqs. (11)–(14).

In the nondegenerate limit, where one has only one electron interacting with the LO phonons of the system, the Fermi occupancy factor n_F in the above equations becomes zero. It is easy to see from Eqs. (5)–(14) that the phonon emission rate at the threshold, $\Gamma_e(k = \gamma)$, then has a discontinuity in two dimensions (unlike in three dimensions), reflecting the constant two-dimensional density of states. In particular, the phonon emission rate at threshold for the strictly two-dimensional system is given by

$$\Gamma_e^{(2D)}(k = \gamma) = \pi\alpha\omega_{LO}(1 + n_B)/2.$$

An accurate approximation to the quasi-two-dimensional system is obtained by multiplying this result with $f(k)$.

At low temperatures, the degenerate case near threshold is very different from the nondegenerate situation just discussed since there are very few empty electronic states available for the electron to decay into, due to Pauli-principle restrictions. The discontinuity in the phonon emission rate at the threshold is considerably suppressed by the Fermi-statistics effect and we get the low-temperature result

$$\Gamma_e^{(2D)}(k = \gamma) \simeq \frac{\pi}{2}\alpha\omega_{LO}e^{-\beta\omega_{LO}}(1 + e^{\beta(\omega_{LO} - \mu)}). \quad (15)$$

For temperatures so low that $\beta\omega_{LO} \gg 1$, we get

$$\Gamma_e^{(2D)}(k = \gamma) \simeq \frac{\pi}{2}\alpha\omega_{LO}e^{-\beta\mu}. \quad (16)$$

Thus the low-temperature phonon emission rate at the threshold is suppressed by a factor of $e^{-\beta E_F}$ due to the effect of degeneracy. For a typical $N_s = 3 \times 10^{11} \text{ cm}^{-2}$ and $T = 50 \text{ K}$ the suppression at threshold is by a factor of 10 for GaAs systems. Since the occupancy factor $(1 + n_B - n_F)$ increases with the electron energy, the two-dimensional emission rate at low temperatures is similar to the three-dimensional result when degeneracy effects are included.

One important effect of degeneracy is that the zero-

temperature threshold energy for phonon emission is shifted from $E_0 = \omega_{LO}$ to $E_0 = E_F + \omega_{LO}$ due to Pauli-principle restrictions. This follows from a simple inspection of the occupancy factors in Eqs. (5)–(14). In particular, the LO-phonon emission rate at $T = 0$ is given by

$$\Gamma_e(E_0) \simeq \frac{\alpha\omega_{LO}^{3/2}}{E_0^{1/2}} f(k) K[(E_0 - \omega_{LO})/E_0]^{1/2} \\ \times H(E_0 - E_F - \omega_{LO}), \quad (17)$$

where $E_0 = k^2/2m$ and we have taken into account the form-factor effect approximately. In Sec. IV we give detailed numerical results without making any analytic approximation.

Most of the above conclusions remain qualitatively valid in the presence of static screening by the free carriers, which we consider next.

III. STATIC SCREENING

Inclusion of screening by free carriers in the above formalism is straightforward if one employs the static random-phase approximation (RPA). Within the static screening approximation, the only modification is that the LO-phonon-mediated effective electron-electron interaction is now screened by the static dielectric function $\epsilon(q, 0)$ so that $f(q)$ in Eq. (1) now changes to $f(q)[\epsilon(q, 0)]^{-2}$. There is also a small renormalization of the LO-phonon frequency which we neglect. Screening is by the square of the dielectric function since the effective electron-electron interaction contains² a product of two electron-phonon interaction vertices, each of which is screened by the free-carrier dielectric function. Equation (11) now changes only by the fact that $f(q)$ in the integrand is replaced by $f(q)[\epsilon(q, 0)]^{-2}$.

The dielectric function $\epsilon(q, 0)$ can be calculated in the RPA, whence

$$\epsilon(q, 0) = 1 - v_C(q)f(q)\Pi(q, 0), \quad (18)$$

where $v_C(q) = 2\pi e^2/\bar{\kappa}q$ is the Coulomb interaction with $\bar{\kappa}$ as the average high-frequency background lattice dielectric constant and $\Pi(q, 0)$ is the static finite-temperature noninteracting polarizability given by²⁴

$$\Pi(q, 0) = - \left[\frac{m}{\pi} \right] \int_0^{1/4} dz \frac{1 - \tanh\{(T_F/2T)[(q^2/k_F^2)z - \mu/E_F]\}}{(1 - 4z)^{1/2}}, \quad (19)$$

where $T_F (= E_F/k_B)$ and $k_F [= (2mE_F)^{1/2}]$ are, respectively, the Fermi temperature and the Fermi wave vector of the system. Equation (19) for the two-dimensional polarizability reduces to the well-known zero-temperature Thomas-Fermi form²⁵ and the high-temperature Debye form²⁶ in the appropriate limits.

All our qualitative discussions for the unscreened situation remain valid in the statically screened case, except that screening further reduces the electron-phonon scattering rate by decreasing the basic electron-phonon in-

teraction strength. Like degeneracy, screening effects are also most pronounced at lower temperatures and higher electron densities. Many of our numerical results presented in the next section are with static screening effects included in the calculation.

One very important theoretical point in the discussion of screening effects is the question of the validity of static screening approximation in dealing with electron-phonon interaction in two-dimensional structures. It has been argued,^{2,27} quite correctly, that static screening may be a

poor approximation in dealing with electron–LO-phonon scattering since LO phonons have comparatively high energies relative to typical electronic energy scales in the system (e.g., plasmon energy or Fermi energy). The problem is further compounded by the fact that the two-dimensional plasma frequency vanishes in the long-wavelength limit, making static screening a poorer approximation in two dimensions compared with the corresponding three-dimensional case.

Our reason for employing a static screening approximation extensively in this paper is twofold: Firstly, it is a well-defined, conceptually simple approximation which has been used²⁸ extensively in dealing with the electron–LO-phonon interaction in three-dimensional, doped semiconductor systems, and, secondly, static screening in overestimating the importance of the screening effect on the electron–LO-phonon interaction gives one an upper bound on how strong screening effects could be (i.e., the actual interaction strength should lie somewhere between the unscreened result and the statically screened result). It has been argued^{29,30} that dynamical screening could give rise to an “antiscreeing” effect, producing a greater scattering rate than the unscreened case. We feel that even though antiscreeing may be effective at *specific* wave vectors (or, equivalently, electron energy), any physical quantity (such as mobility and hot-electron relaxation) involving integrals over energy will not show an antiscreeing effect. In fact, for high electron densities (with consequently high plasma frequency) static screening results should be quite similar to dynamical screening results, as has been shown recently.³¹

Static RPA screening calculations can be shown^{28,31} to be exact in the high-temperature and/or high-electron-density limit (when the plasma frequency is high). The static approximation also works better³¹ for large wave-vector transfers, since the plasmon is damped at large values of the wave vector. In particular, if one takes the typical wave-vector transfer in electron–LO-phonon scattering to be equal to $\gamma = (2m\omega_{LO})^{1/2}$, then the plasma frequency of the electron gas, $\omega_p(q = \gamma)$, is comparable to or larger than the LO-phonon frequency ω_{LO} , making static screening a better approximation than one would have thought otherwise. In particular, the two-dimensional plasma frequency for wave vector γ in the GaAs system for $N_s = 5 \times 10^{11} \text{ cm}^{-2}$ is about 37 meV, which is larger than the LO-phonon frequency ($\omega_{LO} \approx 36 \text{ meV}$).

The best thing would have been to use a dynamical screening approximation to obtain the electron–LO-phonon scattering rates. Such a calculation of the electron–LO-phonon self-energy in the presence of dynamical screening by free carriers has recently been reported³¹ for three- and two-dimensional systems. We want to emphasize the fact that such a calculation cannot be performed within the Fermi golden rule–type one-electron–scattering-rate computations^{29,30} because dynamical screening affects both the LO-phonon frequency (through the hybridized plasmon–LO-phonon modes) and the interaction matrix element. Virtual and real processes involving emission and absorption of coupled plasmon-phonon modes via a dynamically screened

electron-phonon interaction can only be treated in a many-body approach,³¹ as has been presented in this paper.

IV. NUMERICAL RESULTS AND DISCUSSIONS

We will first present the numerical results for the $\text{Al}_x\text{Ga}_{1-x}\text{As-GaAs-Al}_x\text{Ga}_{1-x}\text{As}$ single-quantum-well case. This case is physically simpler within our approximation scheme, where the electron-density effects on the electronic wave function are completely neglected for the quantum-well situation. Thus electron density enters the theory only through the screening effect (and, also through the Fermi occupancy factors) and *not* through the wave-function effect. The main difficulty in depicting the results is the overabundance of independent variables in the problem: electron and lattice temperatures (T_e and T_L), electron density (N_s), well width (a), and electron energy ($E_0 = k^2/2m$). Thus, in principle, one is interested in having numerical results for the LO-phonon emission and absorption rates as a function of five independent variables with and without screening effects (since static screening is a drastically simple approximation whose validity in the electron-phonon interaction calculation remains doubtful except at high temperatures). In Fig. 1 we present our numerical results for the strictly two-dimensional (zero well width) degenerate case without any screening. In Figs. 2–7 we present our numerical results for the LO-phonon emission and absorption rates in quantum-well structures defined, respectively, as Γ_e and Γ_a by Eqs. (2)–(4), both with and without a (static) free-carrier screening effect. We give our results in units of meV, which can be converted to an equivalent “scattering time,” $\tau = \hbar/2\Gamma$, by using the rule $\tau \approx 0.33\Gamma(\text{meV}) \text{ ps}$.

Since the figures are self-explanatory and detailed, we refrain from discussing them individually, but make some general comments about our results.

(1) The electron energy is given as $\epsilon_0 = E_0/\omega_{LO}$, with $(\epsilon_0)^{1/2} = k/\gamma$, where $\gamma = (2m\omega_{LO})^{1/2}$ is the “polaron wave vector.” Note that the electron energy is measured from the bottom of the two-dimensional subband.

(2) Because of the restrictive effects of Fermi statistics, the phonon emission rate is reduced drastically in the en-

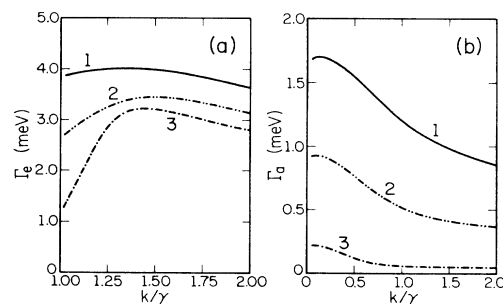


FIG. 1. (a) $\Gamma_e(k)$ for zero well width, $N_s = 3 \times 10^{11} \text{ cm}^{-2}$; (1) $T = 300 \text{ K}$, (2) $T = 200 \text{ K}$, and (3) $T = 100 \text{ K}$; unscreened interaction. (b) $\Gamma_a(k)$, same parameters as (a).

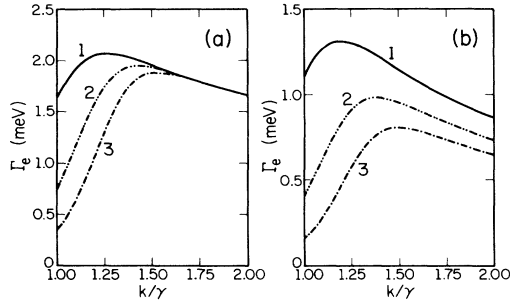


FIG. 2. (a) $\Gamma_e(k)$ for a quantum well, $a = 100 \text{ \AA}$, $T = 100 \text{ K}$; (1) $N_s = 1 \times 10^{11} \text{ cm}^{-2}$, (2) $N_s = 3 \times 10^{11} \text{ cm}^{-2}$, and (3) $N_s = 5 \times 10^{11} \text{ cm}^{-2}$; unscreened interaction. (b) Same as (a) for screened interaction.

ergy region $1 < \varepsilon_0 < 1 + \mu/\omega_{\text{LO}}$, particularly at low electron temperatures and high electron densities (i.e., for small T_e/T_F). Thus, using nondegenerate theory in the situation $T_e/T_F \ll 1$ will give quantitatively incorrect results for the LO-phonon emission rate.

(3) At low temperatures (and/or, high electron densities), the discontinuity in the phonon emission rate at the threshold ($\varepsilon_0 = 1$) is considerably suppressed by the degeneracy effect.

(4) The maximum quantitative effect of screening (compared with the unscreened result) is about a factor of 2 reduction of the scattering rate. As we argued above, static screening is an overestimation of the screening effect and, therefore, screening could, at most, change the calculated polar scattering rate by a factor of 2. Screening effects are particularly important at low temperatures, high densities, and for narrow wells. For $T_e > 50 \text{ K}$ and $a > 150 \text{ \AA}$, screening corrections are of the order of 10–30% for $N_s < 5 \times 10^{11} \text{ cm}^{-2}$. We want to emphasize the fact that at high temperatures a ($T > 200 \text{ K}$) static screening becomes a better approximation and our calculated screening corrections become small. This justifies the use of the unscreened interaction in the calculation of room-temperature mobility limited by polar-optical-

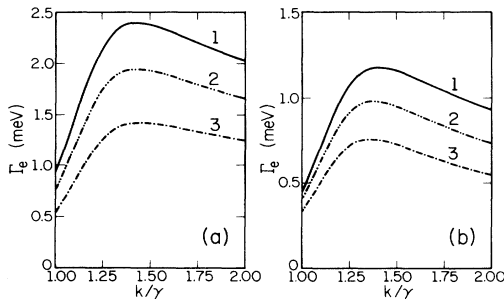


FIG. 3. (a) $\Gamma_e(k)$ for a quantum well, $N_s = 3 \times 10^{11} \text{ cm}^{-2}$, $T = 100 \text{ K}$; (1) $a = 50 \text{ \AA}$, (2) $a = 100 \text{ \AA}$, and (3) $a = 200 \text{ \AA}$; unscreened interaction. (b) Same as (a) for screened interaction.

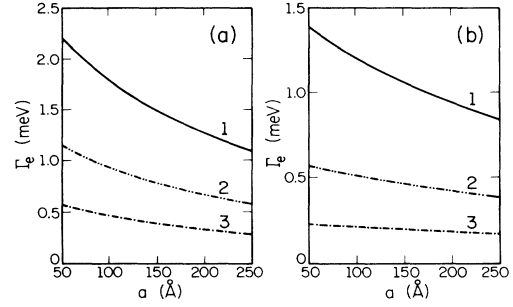


FIG. 4. (a) $\Gamma_e(a)$ for a quantum well, $T = 100 \text{ K}$, $k = 1.05\gamma$; (1) $N_s = 1 \times 10^{11} \text{ cm}^{-2}$, (2) $N_s = 3 \times 10^{11} \text{ cm}^{-2}$, and (3) $N_s = 5 \times 10^{11} \text{ cm}^{-2}$; unscreened interaction. (b) Same as (a) for screened interaction.

phonon scattering, as has been done in some recent publications.¹²

(5) Quasi-two-dimensional wave-function effects are found to be important in all situations and we believe that any quantitative calculation of electron-phonon interaction effects in semiconductor heterostructures must include the form factor arising from electron confinement. We find this to be true at all temperatures ($0 \leq T \leq 300 \text{ K}$) and electron densities ($10^{11} \leq N_s \leq 7 \times 10^{11} \text{ cm}^{-2}$) that we have investigated. Strictly two-dimensional calculations [i.e., $f(q) = 1$] overestimate the interaction strength, whereas three-dimensional calculations may fortuitously be accurate in some situations, but cannot be justified on theoretical grounds since the system is dynamically two dimensional in nature.

(6) Degeneracy has a substantial physical effect on the energy dependence of the LO-phonon emission rate $\Gamma_e(\varepsilon_0)$. For example, as one can see from a typical case like Fig. 2 or 8, the LO-phonon emission rate peaks at a value closer to $E_0 \approx \omega_{\text{LO}} + \mu$ than at ω_{LO} . Thus, even though the discontinuity at the threshold is reduced by occupancy effects, the energy-averaged emission rate may not change much from the nondegenerate situation.

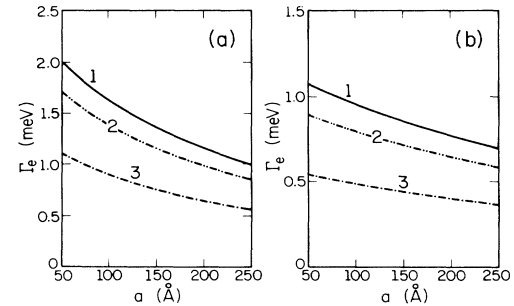


FIG. 5. (a) $\Gamma_e(a)$ for a quantum well, $N_s = 3 \times 10^{11} \text{ cm}^{-2}$, $k = 1.05\gamma$, zero lattice temperature; (1) $T_e = 300 \text{ K}$, (2) $T_e = 200 \text{ K}$, and (3) $T_e = 100 \text{ K}$; unscreened interaction. (b) Same as (a) for screened interaction.

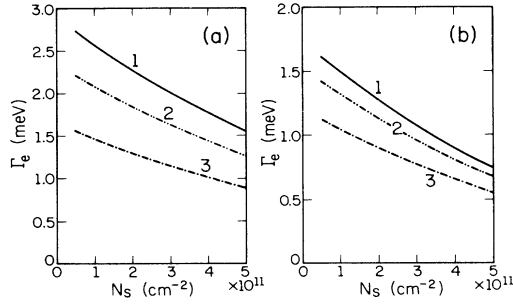


FIG. 6. (a) $\Gamma_e(N_s)$ for a quantum well, $k = 1.05 \text{ \AA}$, zero lattice temperature, $T_e = 300 \text{ K}$; (1) $a = 50 \text{ \AA}$, (2) $a = 100 \text{ \AA}$, and (3) $a = 200 \text{ \AA}$; unscreened interaction. (b) Same as (a) for screened interaction.

Eventually, for very high energies Γ_e falls off again (rather slowly) and degeneracy has a negligible effect in this high-energy region ($E > \omega_{LO} + \mu$). $\Gamma_e(E_0)$ is significantly (and, qualitatively) affected by degeneracy; however, an *energy-averaged* Γ_e may not be. Since an energy-averaged relaxation rate shows up in the hot-electron luminescence experiments, degeneracy effects may average out there and a calculation based on simple nondegenerate theory may produce reasonable results for the hot-electron relaxation rate even when $T_e < T_F$. However, any measurement (e.g., tunneling experiments) that directly probes $\text{Im}\Sigma(E_0)$ should observe significant departure from the nondegenerate theory as our results indicate.

(7) We have used T_e and T_L to denote electron and lattice temperatures, respectively, when these are unequal. Otherwise, $T = T_e = T_L$ denotes the common temperature for both. We want to point out that the phonon occupation factor n_B even for $T_L = 100 \text{ K}$ is only 0.01 and hence our calculated results change by less than 10% between $T_L = 0 \text{ K}$ and $T_L = 100 \text{ K}$ if all the other variables (T_e , N_s , etc.) are kept fixed. Thus all our numerical results for $T < 100 \text{ K}$ could be considered to be hot-electron results with $T_e = T$ and $T_L = 0$.

(8) Since damping due to phonon emission at the

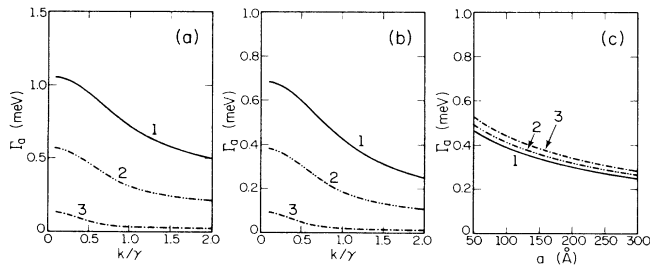


FIG. 7. (a) $\Gamma_e(k)$ for a quantum well, $N_s = 3 \times 10^{11} \text{ cm}^{-2}$, $a = 100 \text{ \AA}$; (1) $T = 300 \text{ K}$, (2) $T = 200 \text{ K}$, and (3) $T = 100 \text{ K}$; unscreened interaction. (b) Same as (a) for screened interaction. (c) $\Gamma_a(a)$ for a quantum well, $T = 300 \text{ K}$, $k = 1.05\gamma$; (1) $N_s = 1 \times 10^{11} \text{ cm}^{-2}$, (2) $N_s = 3 \times 10^{11} \text{ cm}^{-2}$, and (3) $N_s = 5 \times 10^{11} \text{ cm}^{-2}$; screened interaction.

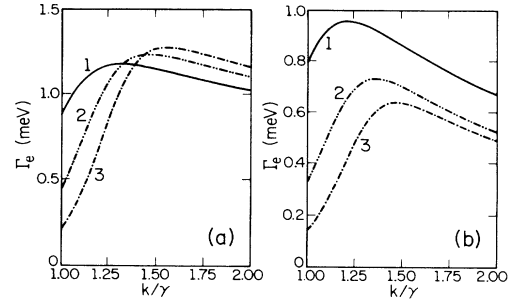


FIG. 8. (a) $\Gamma_e(k)$ for a heterojunction, $T = 100 \text{ K}$; (1) $N_s = 1 \times 10^{11} \text{ cm}^{-2}$, (2) $N_s = 3 \times 10^{11} \text{ cm}^{-2}$, and (3) $N_s = 5 \times 10^{11} \text{ cm}^{-2}$; unscreened interaction. (b) Same as (a) for screened interaction.

threshold is important in some experimental situations, we depict its variation with N_s , T , and a in a number of figures. We define the threshold arbitrarily to be $k = 1.05\gamma$.

The above considerations also apply to our numerical results for the $\text{Al}_x\text{Ga}_{1-x}\text{As-GaAs}$ heterojunction system, which we present next in Figs. 8–12. The main difference between this and the quantum-well case is the dependence of the electronic wave function on the electron density N_s which makes the quantization width (a) a dependent variable. As N_s increases the effective wave function shrinks, making the electron more two dimensional and thus increasing the form factor which tends to enhance the scattering rate. On the other hand, screening also increases with N_s , which tends to decrease the scattering rate. This competition between wave-function and screening effects makes the numerical results less transparent for physical interpretation in the heterojunction situation. At lower N_s the wave-function effect is more important, whereas at higher N_s the screening effect is dominant, so that the self-energy may show an extremum, as we have discussed earlier.⁶ Since N_s and a are dependent variables, we have fewer sets of results for the heterojunction case compared with the quantum-well case. We should remark that the occupancy factors also depend on N_s and, hence, the actual numerical results are quite rich in structure due to competing trends.

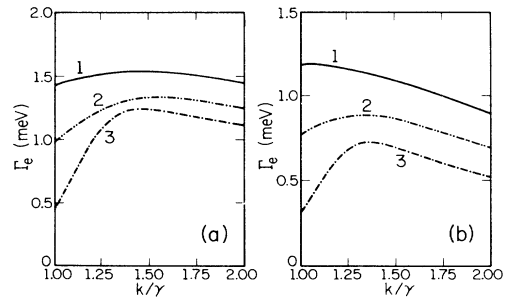


FIG. 9. (a) $\Gamma_e(k)$ for a heterojunction, $N_s = 3 \times 10^{11} \text{ cm}^{-2}$; (1) $T = 300 \text{ K}$; (2) $T = 200 \text{ K}$, and (3) $T = 100 \text{ K}$; unscreened interaction. (b) Same as (a) for screened interaction.

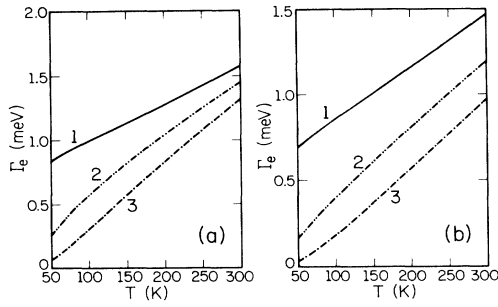


FIG. 10. (a) $\Gamma_e(T)$ for a heterojunction, $k = 1.05\gamma$; (1) $N_s = 1 \times 10^{11} \text{ cm}^{-2}$, (2) $N_s = 3 \times 10^{11} \text{ cm}^{-2}$, (3) $N_s = 5 \times 10^{11} \text{ cm}^{-2}$; unscreened interaction. (b) Same as (a) for screened interaction.

Finally, in Fig. 13 we show a comparative set of hot-electron scattering-rate results for both the quantum-well and heterojunction situations, screened and unscreened. The lattice temperature, in this case, was set to zero and the effective well width of the heterojunction is approximately equal to the quantum-well width. Comparing these figures to previous results, we see that the low lattice temperature has little quantitative effect for electron temperatures below $T_e \sim 150 \text{ K}$. We also see that the polar scattering rate is lower in heterojunctions than quantum wells of similar width.

Due to the very large number of variables involved in the problem, it is not easy to develop a physical feel for our numerical results. We have attempted to give a comprehensive set of results within our approximation scheme. The price one pays for such completeness is a certain lack of precise quantitative statements since Γ depends on many variables, all of which are important in some situations or other. We believe that the figures we give are by far the most complete of any that have been published in the literature on this subject and are self-explanatory. Fairly accurate approximate results can be obtained for the unscreened case by using Eqs. (11)–(14) as explained in Sec. II.

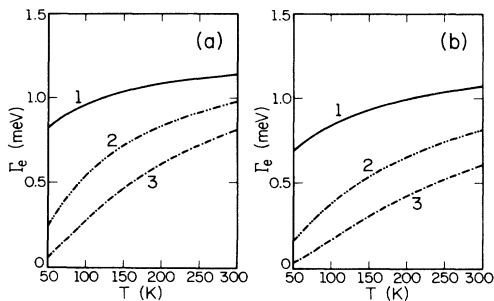


FIG. 11. (a) Same as Fig. 10(a) for zero lattice temperature. (b) Same as Fig. 10(b) for zero lattice temperature.

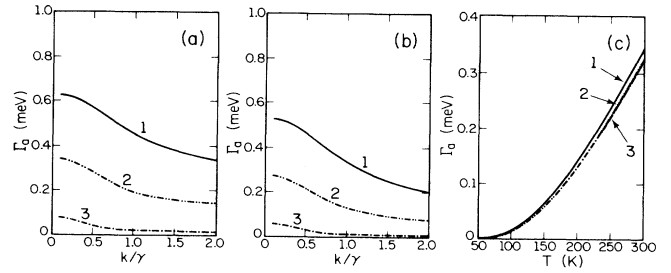


FIG. 12. (a) $\Gamma_a(k)$ for a heterojunction, $N_s = 3 \times 10^{11} \text{ cm}^{-2}$; (1) $T = 300 \text{ K}$, (2) $T = 200 \text{ K}$, and (3) $T = 100 \text{ K}$; unscreened interaction. (b) Same as (a) for screened interaction. (c) $\Gamma_a(T)$ for a heterojunction, $k = 1.05\gamma$; (1) $N_s = 1 \times 10^{11} \text{ cm}^{-2}$, (2) $N_s = 3 \times 10^{11} \text{ cm}^{-2}$, and (3) $N_s = 5 \times 10^{11} \text{ cm}^{-2}$; screened interaction.

V. SUMMARY AND CONCLUSION

In this paper we have provided a rather complete set of numerical results for the electron–optical-phonon scattering in quasi-two-dimensional polar systems such as GaAs quantum wells and heterojunctions. Using a many-body formalism, we calculate the imaginary part of the electronic self-energy to the lowest order in polar coupling. We give detailed numerical results for the LO-phonon

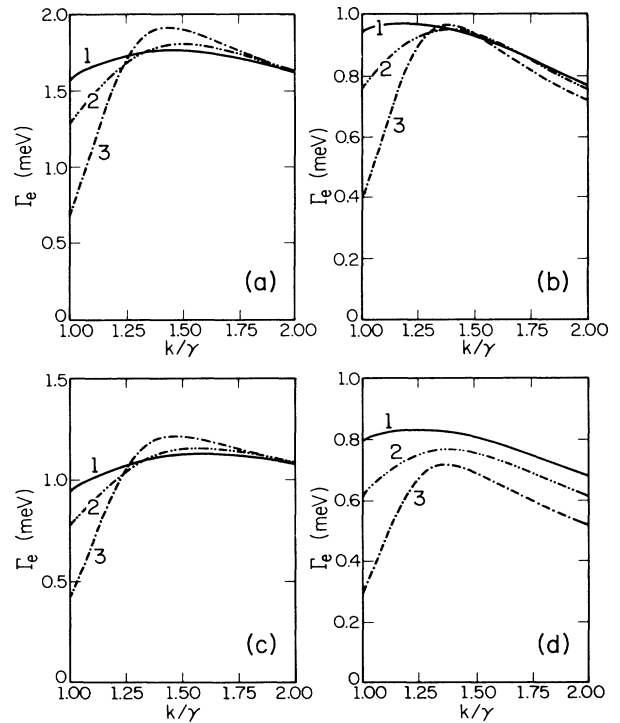


FIG. 13. (a) $\Gamma_e(k)$ for a quantum well, $N_e = 3 \times 10^{11} \text{ cm}^{-2}$, $a = 100 \text{ \AA}$, zero lattice temperature; (1) $T = 300 \text{ K}$, (2) $T = 200 \text{ K}$, and (3) $T = 100 \text{ K}$; unscreened interaction. (b) Same as (a) for screened interaction. (c) Same as (a) for a heterojunction. (d) Same as (b) for a heterojunction.

emission and absorption rates as a function of the electron energy, electron and lattice temperatures, the electron density, and the width of the electron layer.

We give results both for the unscreened case and for the static RPA screening situation. Degeneracy and confining wave-function effects are included in the calculation. Degeneracy effects are important for lower electron temperatures and higher electron densities, whereas wave-function effects are always important.

Our approximation of using the leading-order perturbation theory should be quite good for the weakly polar ($\alpha < 0.5$) semiconductor materials we are interested in. In fact, for GaAs ($\alpha = 0.07$) the leading-order result is essentially exact.² Our use of analytic approximations for the confining electronic wave functions is perhaps less justifiable; however, the quantitative error introduced by these approximations should not be more than 10%. The single-subband approximation is adequate only at low N_s and T when the upper subbands are not appreciably populated. Neglect of intersubband scattering for high values of electron energy is also not justifiable. However, the error arising from these approximations to the calculated polar scattering rates for the parameter values that we actually use in this paper is not thought to be more than 20%, even in the worst situation. In any case, it is straightforward to relax the single-subband approximation and to include numerically the intersubband scattering in the calculation. We believe that our approximation of including electronic coupling only to the bulk GaAs LO-phonon modes is quite valid since the lattice properties of GaAs and $\text{Al}_x\text{Ga}_{1-x}\text{As}$ are very similar.

The most drastic (and, in many ways, the least justifiable) approximation made in this paper is the static screening approximation to calculate the screened polar interaction. This is particularly true at low electron temperatures when dynamical effects of screening should be important. There are two positive statements we can make about the static screening approximation. Firstly, at high electron temperatures the static RPA can be shown to be essentially exact (and a comparison between our statically screened and unscreened polar scattering rates at high T_e shows only about 10% difference, implying weak screening effects at high temperatures anyway). Secondly, our unscreened and statically screened numerical results for the polar scattering rate provide two extreme bounds for the magnitude of the scattering rate since static screening is an overestimation of the actual magnitude of screening corrections. Dynamically screened polar-scattering-rate results fall³¹ somewhere in between the unscreened and statically screened results presented in this paper (of course, it is possible for the dynamically screened result to show additional structures due to plasmon-phonon coupling which are missing in the current work). Results involving dynamical screening will be published elsewhere.³¹

To the best of our knowledge, only very preliminary results for the dynamical screening calculation have yet been reported^{27,31} in the literature. A number of three-dimensional calculations employing static screening exist^{29,32} (and they are claimed to be in fair agreement with experiment). The usual justification for using static

screening in three-dimensional calculations is that in highly degenerate semiconductors the long-wavelength three-dimensional plasma frequency

$$\omega_p(q=0) = [4\pi n e^2 / (\kappa/m)]^{1/2}$$

is usually larger than ω_{LO} . In two dimensions, $\omega_p(q \rightarrow 0) \propto \sqrt{q}$ and, hence, is smaller than ω_{LO} . We believe, however, that the correct plasma frequency to compare is not $\omega_p(q=0)$, but $\omega_p(q=\gamma)$, which could be larger than ω_{LO} in the high-density two-dimensional systems, providing some weak justification for our static RPA screening approximation. Finally, often in situations when an integral over a wave-vector transfer is being evaluated, the important quantity to compare is not the frequency (or the *phase velocity*) of different modes, but the group velocity (i.e., $\partial\omega/\partial q$). Since the plasmon group velocity at small q is very large (varying as $q^{-1/2}$, provided retardation effects can be neglected) and the LO-phonon group velocity is essentially zero, static screening may be much more justifiable³¹ for the calculation of the polar scattering than it appears at first sight.

Experimental information about the polar scattering in two-dimensional structures comes from a number of different measurements, such as mobility measurements at high temperatures, hot-electron studies, and magnetophonon experiments. Unfortunately, each experiment needs its own special theory and the polar scattering rate enters each measurement nontrivially and quite differently. A complete transport theory for a coupled electron-LO-phonon system starting from the Kubo formula does not exist, and the usual approximations for the mobility calculations involve a single-electron approximation and the neglect of screening, in which case the relaxation time defined by

$$(2\tau_t)^{-1} = (\Gamma_e + \Gamma_a) \quad (20)$$

gives the mobility from the simple formula $\mu = e\tau_t/m$ (of course, one must average over energy using the Fermi distribution function in the usual way). Mobility determined in this way accounts for about 80% of the observed resistance of GaAs heterostructures at room temperature and is very close to the corresponding bulk value. Since Mathiessen's rule is not valid at room temperatures, one cannot separate the observed resistivity into contributions from different scattering terms. The relaxation time associated with the hot-electron energy-loss measurements is given by (if phonon absorption effects are completely neglected)

$$(2\tau_e)^{-1} = \Gamma_e \quad (21)$$

and, again, one must average over energy using the Fermi distribution function to obtain a constant-energy relaxation time. It is unclear to us whether such a comparison with experimental results on hot-electron energy loss is meaningful at all,³³ particularly since experimental results¹³⁻¹⁷ disagree with each other. An ideal experiment with which to obtain $\text{Im}\Sigma(E_0)$ directly will be tunneling measurements of the type performed²² by Tsui for the bulk situation. Experiments like tunneling—which are capable of measuring the LO-phonon-induced broaden-

ing of the electronic state—can be compared directly with our theoretical results. Unfortunately, such experimental results for two-dimensional systems are not available at the present time. Our extensive results given in this paper serve as a generalization of the theoretical results given by Conwell³⁴ to degenerate two-dimensional systems. Our results complement earlier studies by Ridley¹¹ and by Price¹⁰ in the sense that we give more complete numerical results with less restrictive approximations (inclusion of degeneracy effects, for example).

ACKNOWLEDGMENTS

One of the authors (S.D.S.) gratefully acknowledges the hospitality of Professor Jörg Kotthaus and co-workers at the University of Hamburg, where this paper was written. This work was supported by the U.S. Army Research Office. We also acknowledge the support of the University of Maryland Computing Center.

APPENDIX

We calculate the form factor $f(q)$ entering Eq. (1) by using analytic approximations^{2,21} to the confining sub-

band wave functions. For the heterojunction, we use the standard Fang-Howard-Stern variational²¹ wave functions, whereas for quantum wells we use the infinite square-well trigonometric wave function.² The ground-state form factor $f(q)$ is then given by

$$f(q) = \begin{cases} \frac{1}{8}(1+qa/3)^{-3}(8+3qa + \frac{1}{3}q^2a^2), & \text{(A1)} \\ 8(q^2a^2+4\pi^2)^{-1} \left[\frac{3}{8}qa + \frac{\pi^2}{qa} - \frac{4\pi^4(q-e^{-qa})}{q^2a^2(q^2a^2+4\pi^2)} \right] & \text{(A2)} \end{cases}$$

where Eqs. (A1) and (A2) refer to the heterojunction and the quantum-well situations, respectively. In Eqs. (A1) and (A2), a is the average thickness of the layer which, for the quantum-well case, is its physical thickness, and, for a heterojunction, is given by $a = (16\pi me^2 N / 9\kappa)^{-1/3}$, where $N = (N_{\text{depl}} + \frac{11}{32}N_s)$ is the effective charge density (N_{depl} being the depletion charge density).

*Present address: Coordinated Science Laboratory, University of Illinois at Urbana-Champaign, Urbana, IL 61801-3082.

†Also at the Institute of Physical Science and Technology, University of Maryland, College Park, MD 20742.

¹For a current status of the field, see the Proceedings of the Sixth International Conference on Electronic Properties of Two Dimensional Systems [Surf. Sci. **170** (1986)].

²S. Das Sarma and B. A. Mason, Ann. Phys. (N.Y.) **163**, 78 (1985).

³S. Das Sarma, Phys. Rev. Lett. **52**, 859 (1984).

⁴S. Das Sarma, Phys. Rev. B **27**, 2590 (1983); Surf. Sci. **142**, 341 (1984).

⁵B. A. Mason and S. Das Sarma, Phys. Rev. B **31**, 5223 (1985).

⁶S. Das Sarma and B. A. Mason, Phys. Rev. B **31**, 5536 (1985).

⁷B. A. Mason and S. Das Sarma, Phys. Rev. B **33**, 1412 (1986).

⁸M. Horst, U. Merkt, and J. P. Kotthaus, Phys. Rev. Lett. **50**, 754 (1983); H. Sigg *et al.*, Phys. Rev. B **31**, 5253 (1985); R. J. Nicholas *et al.*, Phys. Rev. Lett. **55**, 883 (1985).

⁹D. M. Larsen, Phys. Rev. B **30**, 4807 (1984); **30**, 4595 (1984); F. M. Peeters *et al.*, *ibid.* **31**, 3689 (1985); S. Das Sarma and A. Madhukar, *ibid.* **22**, 2823 (1980); R. Lassnig and W. Zawadzki, Surf. Sci. **142**, 388 (1984).

¹⁰P. J. Price, Ann. Phys. (N.Y.) **133**, 217 (1981); Surf. Sci. **113**, 199 (1982); Phys. Rev. B **30**, 2234 (1984); **30**, 2236 (1984).

¹¹B. K. Ridley, J. Phys. C **15**, 5899 (1982); F. A. Riddoch and B. K. Ridley, *ibid.* **16**, 6971 (1983); Physica **134B**, 342 (1985).

¹²W. Walukiewicz *et al.*, Phys. Rev. B **30**, 4571 (1984); K. Lee *et al.*, J. Appl. Phys. **54**, 6432 (1983); K. Hess, Appl. Phys. Lett. **39**, 484 (1979); D. K. Ferry, Surf. Sci. **75**, 86 (1978); T. Drummond *et al.*, J. Appl. Phys. **52**, 5231 (1981).

¹³J. F. Ryan *et al.*, Phys. Rev. Lett. **53**, 1841 (1984).

¹⁴J. Shah *et al.*, Phys. Rev. Lett. **54**, 2045 (1984).

¹⁵C. H. Yang *et al.*, Phys. Rev. Lett. **55**, 2359 (1985).

¹⁶Z. Y. Xu and C. L. Tung, Appl. Phys. Lett. **44**, 692 (1984).

¹⁷J. F. Ryan *et al.*, Surf. Sci. **170**, 511 (1986); J. Shah, J. Quantum Electron. **QE-22**, 1728 (1986).

¹⁸P. J. Price, Physica **134B**, 164 (1985).

¹⁹T. Rahman, P. Riseborough, and D. L. Mills, Phys. Rev. B **23**, 4081 (1981); G. Kawamoto, W. L. Bloss, and J. J. Quinn, *ibid.* **23**, 1875 (1981); S. Das Sarma and A. Madhukar, *ibid.* **22**, 4161 (1980).

²⁰H. Fröhlich, Adv. Phys. **3**, 325 (1954).

²¹See, for example, the extensive review article by T. Ando, A. B. Fowler, and F. Stern, Rev. Mod. Phys. **54**, 437 (1982).

²²D. C. Tsui, Phys. Rev. B **10**, 5088 (1974).

²³S. Engelsberg and J. R. Schrieffer, Phys. Rev. **131**, 993 (1963).

²⁴P. F. Maldague, Surf. Sci. **73**, 296 (1978).

²⁵F. Stern, Phys. Rev. Lett. **18**, 546 (1967).

²⁶A. L. Fetter, Phys. Rev. B **10**, 3739 (1974).

²⁷M. E. Kim, A. Das, and S. D. Senturia, Phys. Rev. B **18**, 6890 (1978).

²⁸H. Ehrenreich, J. Phys. Chem. Solids **8**, 130 (1959); **9**, 129 (1959); G. D. Mahan, in *Polarons in Ionic Crystals and Polar Semiconductors*, edited by J. Devrees (North-Holland, Amsterdam, 1972), p. 553.

²⁹P. J. Price, J. Vac. Sci. Technol. **19**, 599 (1981).

³⁰C. H. Yang and S. Lyon, Physica **134B**, 309 (1985).

³¹S. Das Sarma, A. Kobayashi, and W. Y. Lai, in Proceedings of the 18th International Conference on the Physics of Semiconductors (Stockholm, 1986), and unpublished.

³²J. Collet and T. Amand, Physica **134B**, 394 (1985); A. C. S. Algarte, Phys. Rev. B **32**, 2388 (1985).

³³To make this point explicit, we mention that in three recent experimental publications, Refs. 13, 14, and 15, respectively, the characteristic LO-phonon relaxation time τ_e associated with hot-electron energy-loss measurements in similar GaAs quantum-well structures is given as 6, 1, and 0.15 ps. Our theoretically calculated value is in the range $0.1 \leq \tau_e \leq 1.0$ ps, depending on various parameters (N_s , a , etc.).

³⁴E. Conwell, *High Field Transport in Solids* (Academic, New York, 1963).